

# VCSELs With Optically Controlled Current Confinement

Sven Bader

*We present a concept for optically controlled current confinement in vertical-cavity surface-emitting lasers (VCSELs) based on the monolithic integration of a phototransistor. Omitting the usual oxide aperture improves the manufacturability and prevents built-in strain near the active zone. Measured continuous-wave operation characteristics of fabricated devices show hysteresis loops in the current-voltage and light-current curves or a negative differential resistance region. Requirements for the switch-on point of the laser are defined and explained.*

## 1. Introduction

Vertical-cavity surface-emitting lasers are widely used in optical sensing and short-distance data communication [1]. Two major advantages of these devices compared to conventional edge-emitting laser diodes are low threshold currents and high conversion efficiencies at low output power. This requires high current densities in the close proximity of the active region via current confinement. Early demonstrations successfully used mesa etching [2] and proton implantation [3]. Epitaxial regrowth is an alternative method to produce current-blocking regions [4, 5].

The bulk of today's commercial VCSELs relies on oxide confinement [1, 6], where excellent operation behavior is achieved. Using a wet-thermal oxidation process, AlGaAs layers of the top mirror with very high aluminum content are turned selectively into a non-conductive oxide and thus form buried apertures. A tight process control is required for reproducible results. During oxidation, the volume of the AlGaAs layers shrinks. Hence, strain near the active zone of the VCSEL is inevitable, which gives rise to concerns about the very-long-term reliability of the laser [7].

In order to avoid these disadvantages, we have developed a novel approach for current confinement [8]. In contrast to existing methods, the concept is based on the idea that the laser light beam itself should determine the current path through the device. Therefore a phototransistor (PT) is monolithically integrated close to the active region of the VCSEL. Only light-exposed PT areas allow current flow, whereas un- or underexposed regions form a current-blocking layer (Fig. 1). Hence, the PT works as an optical switch. This should result in an optically controlled enhancement of the current density distribution in close vicinity to the laser mode.

The article is organized as follows. Section 2 introduces the novel current confinement concept in some detail. Continuous-wave (cw) measurements of fabricated devices are presented in Sect. 3. A model of the turn-on behavior is presented in Sect. 4.

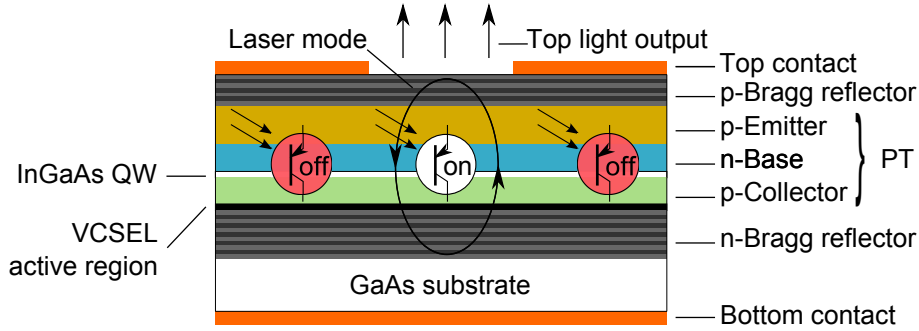


**Fig. 1:** Layout and operation principle of a top-emitting oxide-free PT-VCSEL with optically controlled current confinement. The integrated phototransistor, consisting of emitter, base, and collector layers, is configured as an optical switch. Areas exposed to the laser beam turn conductive, which results in a laterally defined current path.

## 2. Device Concept

Previous methods achieving current confinement in VCSELs manipulate the current flow with physical barriers which form non-conductive layers. In consequence, the laser beam is affected directly by the current path and will establish at areas with the highest current density. The concept presented here works oppositely. The photons of the VCSEL beam specify the current path, which entails an optical feedback. This is enabled by epitaxially integrating a PT on top of the active region of the VCSEL between the two Bragg reflectors (Fig. 1). In the standard configuration, the PT works similar to a bipolar transistor, here pnp-type, which means that it consists of p-emitter, n-base, and p-collector layers. In PTs, a photocurrent  $I_{\text{ph}}$  is generated by absorption of incident photons in the base–collector depletion zone. In the devices discussed below, for this task an InGaAs quantum well (QW) with defined width  $d$  and absorption coefficient  $\alpha$  is embedded between base and collector. The photocurrent is equivalent to the base current  $I_{\text{B,ph}}$  which controls the collector current flow through the device. Thus, no external base current is needed. The generated base current can be estimated accordingly as

$$I_{\text{B,ph}} \hat{=} I_{\text{ph}} = (1 - \exp(-\alpha d)) \cdot \frac{q\lambda}{hc} \cdot P \approx \alpha d \cdot \frac{q\lambda}{hc} \cdot P \quad (1)$$

like in a regular pin-type photodiode, where the approximation is valid for  $\alpha d \ll 1$  (as in a QW).  $q$  is the elementary charge,  $h$  is Planck's constant, and  $c$  the vacuum velocity of light. Incident light emitted from the VCSEL's active region, with wavelength  $\lambda$  and power  $P$  in the cavity is responsible for  $I_{\text{B,ph}}$ , which means that the coupling between VCSEL and PT creates an optical feedback. The laser is driven by an external current  $I_0$ , which can only flow in the light-exposed areas. There, the electrons of the photocurrent are swept directly through the n-doped base toward the p-emitter layer. Due to the charge neutrality of the base, the hole current  $I_0$  flows through the device toward the collector. To reach this state, a certain amount of photons are required to satisfy the turn-on condition, which is introduced and explained in detail in Sect. 4. Un- or underexposed areas remain non-conductive when the optical power is too small and hence not able to switch the PT on. In this new concept, the lateral position of the laser beam cannot be influenced by

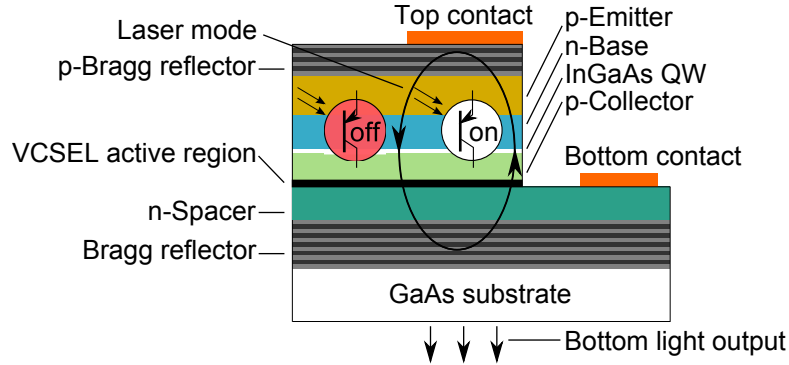


**Fig. 2:** Schematic layer structure of the investigated bottom-emitting PT-VCSEL.

just controlling the current path. Instead, the photons and hence the location of the laser mode must be manipulated directly by the quality of the resonator. The laser field will establish where the best cavity is found, as defined, e.g., by the top contact metal or a shallow surface relief [9]. As shown in Fig. 1, no transverse waveguiding is provided.

One-step epitaxial growth plus metal deposition can already produce a fully functional VCSEL. No mesa-etching and oxidation are required, which prevents the mentioned built-in strain near the active zone. The low additional structural complexity and the inherent light-to-current alignment give this device a strong potential to simplify the fabrication. The latter feature should also be beneficial for the conversion efficiency of such devices.

### 3. Characterization

#### 3.1 Bottom-emitting PT-VCSEL

We have grown first test structures by molecular beam epitaxy. The schematic layer structure is depicted in Fig. 2. The active zone contains three InGaAs QWs for lasing operation at  $\lambda = 1040$  nm. The PT layers are made of GaAs and are 255 nm thick. The 6 nm thick absorbing QW of the PT, embedded between the base and collector layer, has an absorption coefficient of  $\approx 3500$  cm<sup>-1</sup>. The resonator is formed by 4 AlGaAs–GaAs-based top mirror pairs and 31.5 binary (AlAs–GaAs) mirror pairs of the bottom reflector with a simulated lossless reflectivity of  $R_{\text{bottom}} = 99.99\%$ . The VCSEL was processed for light output through the thicker mirror because the laser mode establishes under the top contact metal (Ti/Pt/Au) due to the increased top mirror reflectivity. The estimated threshold gains are 2750 cm<sup>-1</sup> (corresponding to  $R_{\text{top}} = 99.3\%$ ) and  $\approx 37000$  cm<sup>-1</sup> ( $R_{\text{top}} = 74.6\%$ ) with and without the metal, respectively.

Figure 3 (a) shows the measured light–current–voltage (LIV) characteristics of the PT-VCSEL bottom emitter when the current is ramped from 0 to 3.5 mA. Owing to this initial, non-ideal design, the optical output power is rather low. For very low input currents below 20  $\mu$ A (point A), the IV curve corresponds to the usual dark current ( $I_{\text{B,ph}} = 0$ ) region of a PT, where the current results from the leakage current of the collector–base junction. Above 20  $\mu$ A the curve shows a negative differential resistance (NDR) behavior until

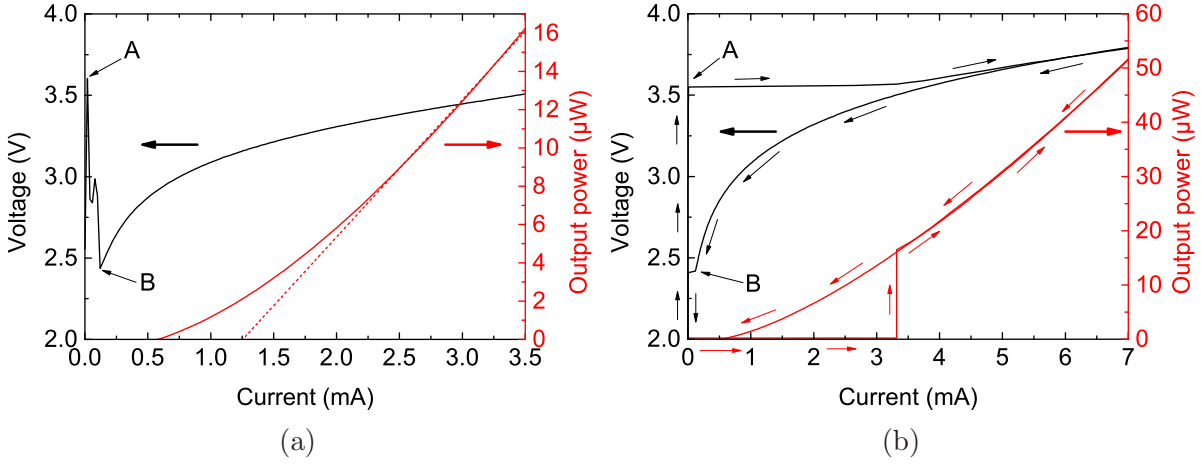


**Fig. 3:** Continuous-wave operation curves of the device from Fig. 2 when ramping (a) the current or (b) the voltage, which results either in an NDR region or a hysteresis loop. The operation points A and B are addressed in the text. The linear fit (dashed line in (a)) serves to estimate the threshold current.

120  $\mu\text{A}$  (point B). At this point the PT switches on. A further current increase results in lasing operation above the threshold current  $I_{\text{th}} = 1.26 \text{ mA}$ . CCD camera observations qualitatively show that the positive curvature of the LI curve is caused by an expansion of the laser mode diameter since there is no built-in transverse waveguiding, in contrast to oxide-confined VCSELs. For PT-VCSELs a behavior similar to gain-guided VCSELs can be expected, with contributions from thermally induced index guiding. The current confinement in this device is thus rather weak.

Driving the PT-VCSEL with a voltage ramp, the switch-on/-off behavior changes into a hysteresis loop (Fig. 3 (b)). First, as for current ramping, the device is operated on the identical dark current curve. At 3.55 V (point A) the current increases suddenly to 3.32 mA and the device turns on. Once  $I_{\text{B,ph}}$  flows through the device, the current rises in a positive feedback loop (more collector current induces more light emission in the QWs, which means more absorption in the PT and thus a higher  $I_{\text{B,ph}}$ ) until reaching the stable state at the diode characteristic curve of the PT-VCSEL. Reducing the voltage, the laser remains on the diode curve (due to the already conductive base) until the PT turns off at 2.42 V with a remaining current of 120  $\mu\text{A}$  (point B).

The LIV characteristics in Figs. 3 (a) and (b) differ only in the switch-on/-off mechanism of the PT. After leaving operation on the dark current curve due to  $I_{\text{B,ph}} > 0$ , the NDR region originates from an unstable state where not enough photons are available to switch the PT on. In contrast, while using a voltage source, the PT jumps directly to the on-state of the PT and the VCSEL. Ramping down from lasing operation, in both cases the LIV characteristics are identical up to the switching point of the PT. Using a current source the device enters the NDR region again, whereas with a voltage source the IV curve suddenly jumps to the dark current curve. Thus, this behavior results in a hysteresis loop.

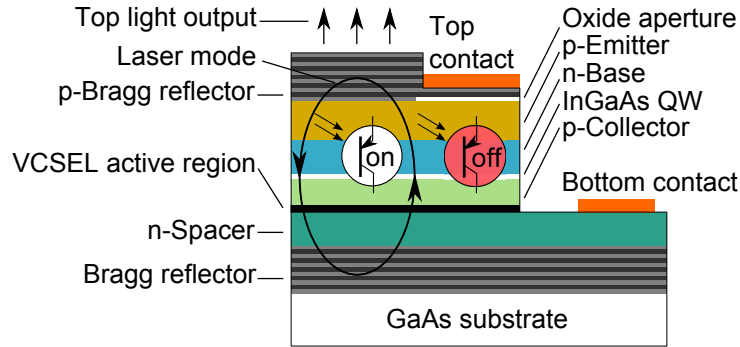


**Fig. 4:** Layer structure of the top-emitting PT-VCSEL. The oxidized aperture avoids laser operation under the top contact.

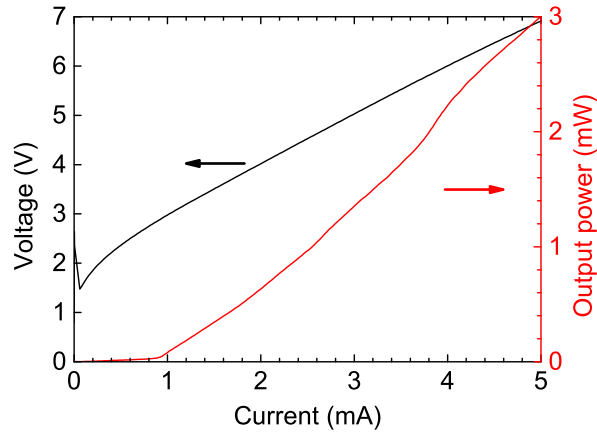


**Fig. 5:** LIV characteristics of the top-emitting PT-VCSEL with current ramping.

### 3.2 Top-emitting PT-VCSEL

In order to increase the optical output power, the device from Fig. 2 has been post-processed to create a top emitter (Fig. 4): First, we applied dielectric mirror layers which increase the top mirror reflectivity to 98.9%. Second, an oxide aperture with  $9\ \mu\text{m}$  diameter was incorporated between the top mirror and the emitter layer. The oxide width was chosen according to the contact width to prevent lasing under the contact. The LIV characteristics are depicted in Fig. 5. The current was ramped from 0 to 5 mA.

As expected, the optical power of the device increases drastically to the mW range. The threshold current amounts to 0.90 mA. The average slope efficiency is about  $0.77\ \text{W/A}$ , which is 70 times higher than that of the bottom emitter. Lasing starts at the fundamental mode. With increasing current, higher-order modes begin to oscillate, which is visible as a kink in the LI curve at 3.7 mA. The NDR region at very low currents proves the functionality of the PT and hence its predicted influence on the current confinement. Nevertheless the current confinement is rather weak because the current aperture grows with increasing current. This can be improved by decreasing the photosensitivity of the PT. Raising the transparency of the InGaAs QW will enhance the slope efficiency in an improved design.

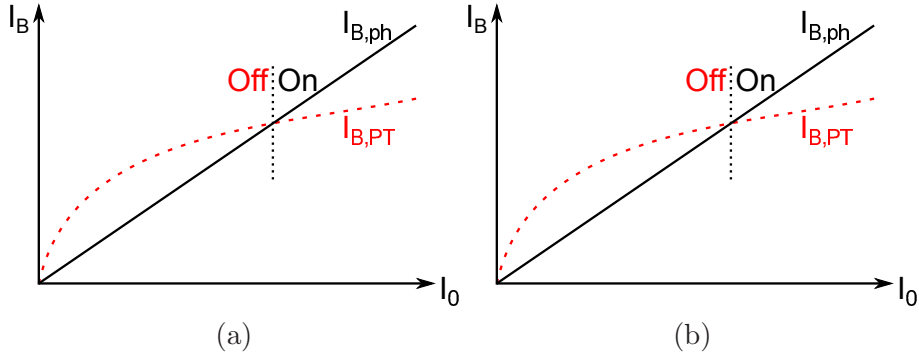


**Fig. 6:** Graphical illustration of the base photocurrent  $I_{B,ph}$  and of  $I_{B,PT}$  versus the laser current  $I_0$ . The point of intersection defines the switching point of the PT determined by (a) the nonlinear shape of the gain curve of the PT at low currents in the  $\mu\text{A}$ -range and (b) the threshold current of the PT-VCSEL (mA-range). Operation according to (b) is desired for strong current confinement.

#### 4. Turn-on Model

As mentioned in Sect. 3, the turn-on current and voltage largely define the current confinement functionality of the device. They depend on several parameters, namely the absorption coefficient  $\alpha$  of the absorbing layer of the PT, its position in the standing-wave field in the cavity, as well as the current gain  $\beta_{PT}$  of the PT.

The latter determines the laser (or collector) current  $I_0$  via the base current according to

$$I_0 = \beta_{PT} \cdot I_{B,PT}, \quad (2)$$

where  $I_{B,PT}$  defines the base current which is needed to turn the PT on in order to allow  $I_0$  to flow through the laser. If a current  $I_0 < I_{th}$  is provided by a current source, spontaneous optical power  $P_{se}$  is generated in the active region of the VCSEL, where  $P_{se} \propto I_0$  like in a light-emitting diode. Identifying  $P = P_{se}$  we obtain  $I_{B,ph} \propto \alpha d \cdot I_0$  from (1). Hence the base current  $I_{B,ph}$ , created by absorption, is not constant but depends linearly on  $I_0$ . According to (2) this is also valid for  $I_{B,PT}$ . However, in a regular transistor  $\beta_{PT}$  turns out to be not constant while increasing  $I_0$ , which directly affects the slope of  $I_{B,PT}$  versus  $I_0$ , as sketched in Fig. 6 (a). Low collector currents result in low current gains due to high recombination currents in the emitter–base depletion zone and interface and possibly surface leakage currents. This behavior is known and well explained in the literature using the so-called Gummel plot [10]. The PT switches to the on-state when  $I_{B,ph} \geq I_{B,PT}$ , which ensures the current flow  $I_0$  through the laser. While increasing  $I_0$  from the dark current curve ( $I_{B,ph} = 0$ ) toward the turn-on point, the NDR region appears since the device transitions from an off-state with high voltage to a low-resistance on-state.

The turn-on point can be graphically determined by plotting  $I_{B,ph}$  and  $I_{B,PT}$  versus  $I_0$ . The point of intersection of both lines defines the turn-on current where  $I_{B,ph} = I_{B,PT}$  is satisfied. Due to the effect of the nonlinear  $\beta_{PT}$  at low  $I_0$ , the point of intersection is located at low currents. However, if  $\beta_{PT}$  was constant, no such defined turn-on effect of the device would be expected. To achieve strong optically controlled current confinement, this point should be shifted to the threshold current  $I_{th}$  of the VCSEL. Otherwise, low currents,

respectively low optical powers, are sufficient to switch the PT on, which is likely to lead to a lateral broadening of the laser field when the evanescent tails of the laser mode(s) are able to open the PT. This corresponds to a weak current confinement, as seen in the experiments in Sects. 3.1 and 3.2. Figure 6 (b) depicts the desired operation. The PT should be in the off-state until  $I_{\text{th}}$  is reached. This could be achieved by reducing its current gain. Simultaneously, the PT should be designed to have a lower light sensitivity by decreasing the absorption coefficient of the InGaAs QW in the present design or by shifting its position towards a field node in the resonator. After finally reaching  $I_{\text{th}}$ , the amount of photons and hence  $I_{\text{B,ph}}$  will rise strongly due to stimulated emission. This would lead to a turn-on point slightly beyond  $I_{\text{th}}$  (see Fig. 6 (b)) and therefore to strong optically controlled current confinement.

## 5. Conclusion

In summary, we have presented the concept of a novel oxide-free VCSEL with optically controlled current confinement induced by a monolithically integrated phototransistor next to the laser active region. First experiments give clear indications of the functionality of the transistor in both operation schemes: in current mode, a negative differential resistance region appears in the IV curve and in voltage mode, wide hysteresis loops establish both in the IV and LI curves. We have introduced a simple model to explain the occurrence of a distinct turn-on point of the PT-VCSEL. After the PT has turned-on, regular VCSEL behavior is found.

In the fabricated initial devices, the degree of current confinement is smaller than desired. This can be deduced from the continuous increase of the slope of the LI curve resulting from an expansion of the beam diameter, which is observed on qualitative images of the mode profile. The waveguiding properties of PT-VCSELs will be a topic of future studies. Also a noticeable voltage penalty is caused by the present design of the PT. We have indicated the routes to optimize these adverse effects, namely a higher transparency of the absorbing QW and a reduction of the PT's current gain. Implementing these, there is a strong potential to create a new kind of high-performance VCSELs with simplified fabrication and potentially superior reliability.

## Acknowledgment

The author thanks Philips Technologie GmbH (U-L-M Photonics) for the MBE growth and the contributions to the processing of the PT-VCSELs. Furthermore the author is grateful to Dr.-Ing. Philipp Gerlach for the numerous helpful discussions and the food for thoughts. Also the author acknowledges the technical support of Susanne Menzel and Rudolf Rösch.

## References

- [1] R. Michalzik (Ed.), *VCSELs — Fundamentals, Technology and Applications of Vertical-Cavity Surface-Emitting Lasers*, Springer Series in Optical Sciences, vol. 166. Berlin: Springer, 2013.
- [2] J.L. Jewell, A. Scherer, S.L. McCall, Y.H. Lee, S. Walker, J.P. Harbison, and L.T. Florez, “Low-threshold electrically pumped vertical-cavity surface-emitting micro-lasers”, *Electron. Lett.*, vol. 25, pp. 1123–1129, 1989.
- [3] M. Orenstein, A.C. Von Lehmen, C. Chang-Hasnain, N.G. Stoffel, J.P. Harbison, L.T. Florez, E. Clausen, and J.E. Jewell, “Vertical-cavity surface-emitting InGaAs/GaAs lasers with planar lateral definition”, *Appl. Phys. Lett.*, vol. 56, pp. 2384–2386, 1990.
- [4] M. Ortsiefer, W. Hofmann, J. Roskopf, and M.C. Amann, “Long-Wavelength VCSELs with Buried Tunnel Junction”, Chap. 10 in *VCSELs*, R. Michalzik (Ed.), pp. 321–351. Berlin: Springer, 2013.
- [5] X. Yang, M. Li, G. Zhao, Y. Zhang, S. Freisem, and D. Deppe, “Small-sized lithographic single-mode VCSELs with high power conversion efficiency”, *Proc. SPIE*, vol. 9381, pp. 93810R-1–6, 2015.
- [6] D.L. Huffaker, D.G. Deppe, K. Kumar, and T.J. Rogers, “Native-oxide defined ring contact for low threshold vertical-cavity lasers”, *Appl. Phys. Lett.*, vol. 65, pp. 97–99, 1994.
- [7] B.M. Hawkins, R.A. Hawthorne III, J.K. Guenter, J.A. Tatum, and J.R. Biard, “Reliability of various size oxide aperture VCSELs”, in *Proc. Electron. Comp. and Technol. Conf. (ECTC)*, vol. 52, pp. 540–550, 2002.
- [8] S. Bader, P. Gerlach, and R. Michalzik, “Novel oxide-free VCSEL with optically controlled current confinement”, *Europ. Conf. on Lasers and Electro-Optics, CLEO/Europe*, paper CB-2.6, one page, 2015.
- [9] H.J. Unold, S.W.Z. Mahmoud, R. Jäger, M. Grabherr, R. Michalzik, and K.J. Ebeling, “Large-area single-mode VCSELs and the self-aligned surface relief”, *IEEE J. Select. Topics Quantum Electron.*, vol. 7, pp. 386–392, 2001.
- [10] S.M. Sze, “Bipolar Transistors”, Chap. 3 in *Physics of Semiconductor Devices*, pp. 133–189, New York: John Wiley and Sons, 1981.